

# Microfabricated out-of-plane arrays of integrated capillary nano-electrospray emitters

IEPC-2009-188

*Presented at the 31st International Electric Propulsion Conference,  
University of Michigan • Ann Arbor, Michigan • USA  
September 20 – 24, 2009*

Renato Krpoun<sup>1</sup> and Herbert R. Shea<sup>2</sup>  
*Ecole Polytechnique Fédérale de Lausanne (EPFL), 2002 Neuchâtel, Switzerland*

We present the fabrication and operation of an integrated nano-electrospray thruster consisting of an array of microfabricated silicon capillary emitters and microfabricated silicon extractor electrodes. Based on previous work in which we showed operation of single microfabricated capillaries, the improved microfabricated thruster presented here allows simultaneously operation of arrays of emitters. In addition, we control the hydraulic impedance of the capillaries by filling them with silica beads, thus tailoring the flow rate in order to spray either in droplet regime or in ionic regime for two ionic liquids (EMI-BF<sub>4</sub> and EMI-Im). Operation in both modes is confirmed by mass spectrometry and retarding potential analysis. In ion regime, a specific impulse of 3500 s is obtained at 1.2 kV for the ionic liquid EMI-BF<sub>4</sub>.

## I. Introduction

THE recent discovery<sup>1</sup> of an electrospray emission regime in which ions instead of droplets are emitted has sparked interest to use electrospray sources for applications such as spacecraft propulsion<sup>2</sup> or for surface micro-machining<sup>3</sup>. Because the mass throughput of electrosprays in ionic mode is very low, one single emitter is insufficient to generate the necessary mass throughput to generate sufficient thrust even for picosatellite missions, hence the need for arrays of emitters.

Pure ion mode has previously only been shown with externally wetted emitters<sup>4</sup> and single, macroscopic capillaries<sup>1</sup>. We present here the microfabrication and testing of arrays of 19 capillaries that can be operated in either pure ion mode or in droplet mode depending on the applied voltage and on the hydraulic impedance of the silicon capillaries.

## II. Device fabrication and assembly

Figure 1 shows the layout of our thruster consisting of a micromachined array of Silicon capillaries and extractor electrodes, each etched from an SOI wafer, passively aligned, and mounted on a ceramic support providing fluidic and electrical interfaces, as well as integrated heaters and temperature sensors.

Figure 2 is an SEM image of the assembled capillaries with integrated extractor electrodes providing an individual extractor aperture for each emitter. Extractor and capillary chips are separated by ruby balls serving as insulators and alignment features, proving 2  $\mu\text{m}$  in-plane alignment accuracy. By suitable choice of ruby ball diameter, the electrode to emitter spacing can be adjusted, for the results reported hereafter the distance was fixed at 90  $\mu\text{m}$ . Figure 3 is an image of one single capillary, with a stand-off height of 70  $\mu\text{m}$  and an external diameter of 34  $\mu\text{m}$  at the tip. The detailed process flow is given in reference 5, and is based in part on the fabrication sequence developed in reference 6. The array pitch is 250  $\mu\text{m}$ , for a density of 1800 capillaries/cm<sup>2</sup>. Each emitter has its own extraction electrode, to ensure the same electric field is applied to each emitter, making onset voltage much more uniform between emitters.

---

<sup>1</sup> Dr. Krpoun is now project manager at CSEM Brasil. email: renato.krpoun@csembrasil.com.br

<sup>2</sup> Professor, Microsystems for Space Technologies Laboratory, email: herbert.shea@epfl.ch

A key innovation to both prevent flooding and to enable operation in ion mode for this geometry is the addition of a controllable fluidic impedance, in the form of silica microspheres with which the capillary is filled. The microspheres are introduced into the capillaries by placing a drop of microspheres dispersed in a water/isopropyl solution on the back of the capillary chip. This solution is passively pulled into the capillaries through capillarity. Once dried, the microspheres are fixed together through a silanization process. Figure 4 shows a detail of the fixed spheres, here with a  $4.74\ \mu\text{m}$  average diameter. Beads of diameter  $1\ \mu\text{m}$  and  $2\ \mu\text{m}$  were also successfully used.

The stack of two SOI wafer is connected to a pressurized ionic liquid reservoir by means of an Upchurch Scientific NanoPort attached to the backside of the LTCC interface, as shown in Figure 5. The LTCC chip allows sensing of the liquid presence, measuring the temperature, and heating. Figure 6 shows the fully integrated thruster clamped between stainless steel and PEEK elements. The chip can be easily disassembled after spraying for analysis, e.g., of possible erosion or droplet accumulation.

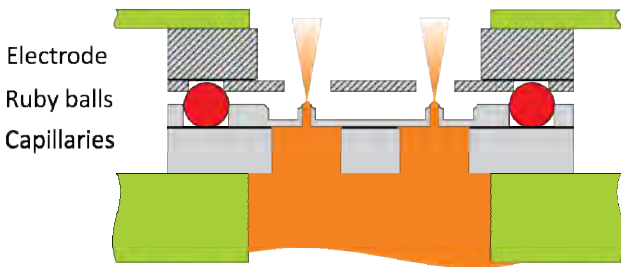


**Figure 1: Schematic cross section of the assembled thruster. The extractor electrode is bonded on the capillary chip (emitter) spaced by ruby balls. The capillary chip and a fluidic interface are glued onto a ceramic support through which the fuel is fed.**

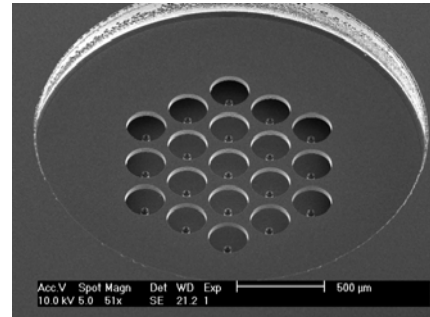


**Figure 2: SEM image of an assembled microfabricated colloid thruster consisting of 19 micromachined capillaries and extractor electrodes (here the extractors are all at the same potential).**

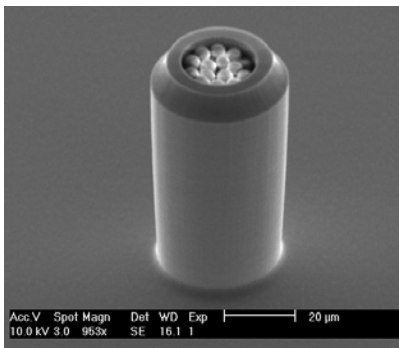


**Figure 3: SEM photograph of a single capillary filled with  $5\ \mu\text{m}$  silica microspheres to increase hydraulic impedance. The stand-off height of the capillary is  $70\ \mu\text{m}$  and the inner diameter is  $24\ \mu\text{m}$ .**

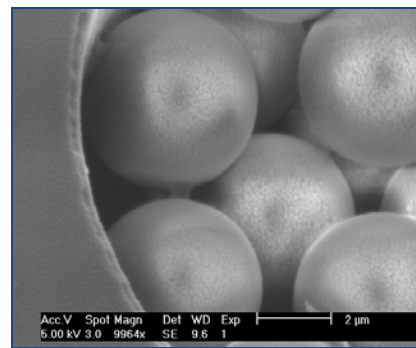


**Figure 4: SEM image the silica beads, linked by a grown  $\text{SiO}_x$  film, visible as the link between beads, holding the them in place to prevent their emission during electrospray. Processing details can be found reference 5.**

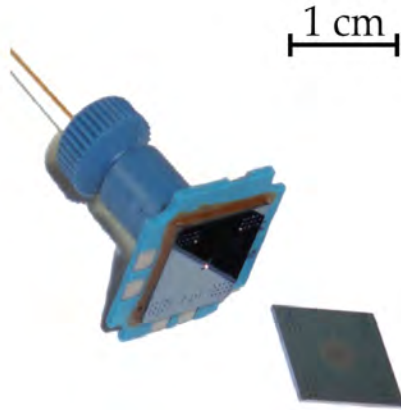


Figure 5: MEMS thruster head on LTCC holder and Upchurch Scientific NanoPort showing fluidic interface.

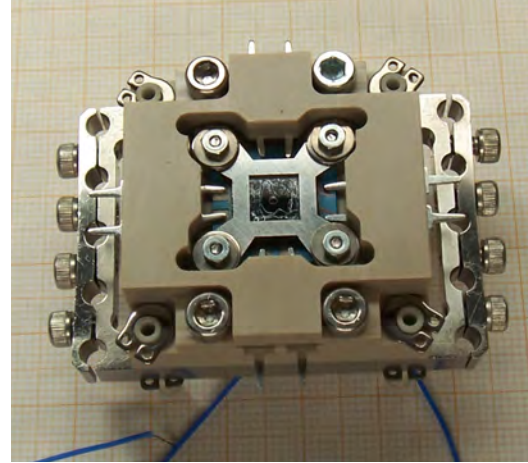


Figure 6: MEMS thruster head integrated into holder proving electrical and mechanical interfaces.

### III. Testing of the electro spray array

Testing was carried out in vacuum (base pressure  $<3.10^{-7}$  mbar) for both single capillaries and arrays of 19 capillaries. The capillary emitters were placed at high voltage while the extractor electrode was grounded. Spray current was measured using a Faraday cup, equipped with retarding potential grids. Spray tests successfully were carried out with the ionic liquids EMI- $\text{BF}_4$  and EMI- $\text{Tf}_2\text{N}$  (often referred to as EMI-Im). As recommended by Lozano *et al.*<sup>8</sup> the polarity was switched periodically (0.2 to 1 Hz) to avoid electrochemical reactions.

Figure 7 shows the measured emitter spray current as a function of time during a peak to peak 2 kV voltage square wave for an array of 19 capillaries filled with 5  $\mu\text{m}$  diameter silica beads for EMI- $\text{Tf}_2\text{N}$  (also known as EMI-Im). Figure 8 shows the effect of the microbeads on beam current. With no beads, the electro spray current increases with emitter voltage. However for capillaries with microspheres, a decrease in current is observed above 1100 V. This observation matches earlier measurements done with macroscopic capillaries spraying EMI- $\text{BF}_4$  as in reference 7. One possible explanation for this behavior is that at higher electric pressure the operating mode transitions to a higher droplet fraction, which in general carries less current for a given backpressure. We explain below how we determine that below 1100 V, the emitter with microbeads is operating principally in ion mode, and switches to a droplet mode at higher voltages (hence higher flowrates).

To determine the energy distribution of the particles in the emitted beam, a retarding voltage  $V_{\text{RP}}$  was applied to a grid placed in front of the Faraday cup. Figure 9 shows the evolution of the density distribution as a function of emitter potential. One main peak can be seen at an energy deficit of 120 V. These results correspond to measure-

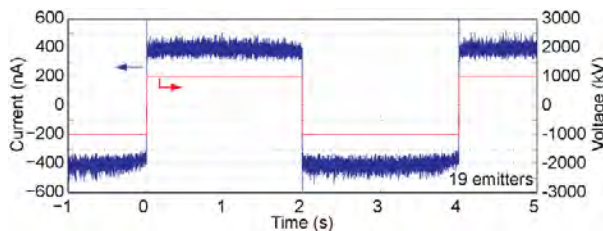


Figure 7: Current emitted from a 19 emitter capillary array using the ionic liquid EMI- $\text{Tf}_2\text{N}$  as fuel.

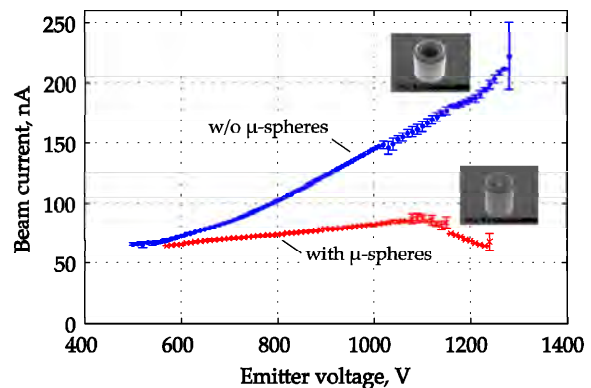
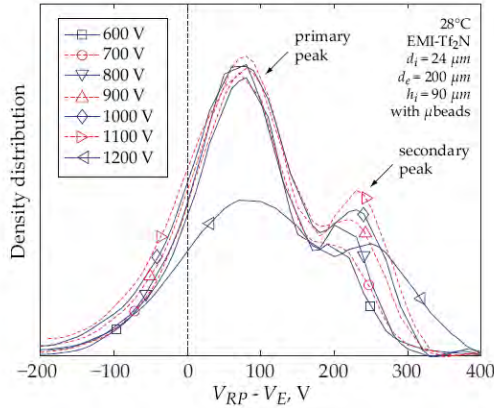
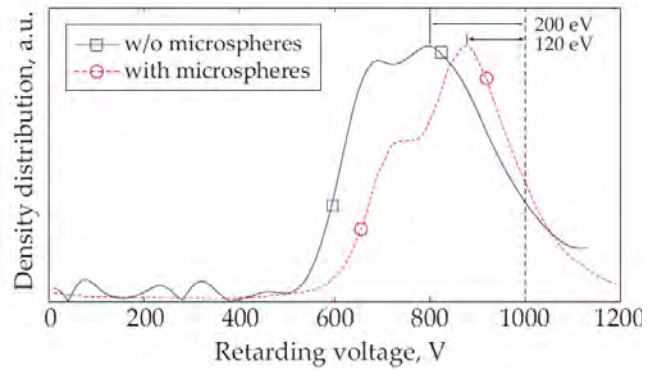


Figure 8: I-V curves for a single capillary with and without microspheres (fuel EMI- $\text{Tf}_2\text{N}$ ).<sup>9</sup>



**Figure 9: Retarding potential density distribution measurements for a 24  $\mu\text{m}$  i.d. capillary filled with 5  $\mu\text{m}$  microbeads spraying EMI-Tf<sub>2</sub>N. The emitter voltage is subtracted from the retarding voltage to show the similarity of energy distributions for different emitter voltages. A change in beam properties is clearly visible above 1100 V.**



**Figure 10: Energy density distribution contrasting emitters with and without microbeads, when spraying the liquid EMI-Tf<sub>2</sub>N. The smaller energy deficit and narrower energy distribution for the capillaries with microspheres indicate ionic operation, and the broader deficit mixed ion/droplet mode<sup>9</sup>.**

ments by other groups using single non-micromachined capillaries, suggesting ionic mode operation, with the second bump possible corresponding to the presence of droplets (230 V deficit), as reported by Gamero-Castaño<sup>10</sup>. We interpret the curves as corresponding to pure ionic regime up to 1100 V, while above 1100 V mixed ion-droplet emission sets in. We observed this behavior on single capillaries and on arrays of 19 capillaries with a density 1800 capillaries/cm<sup>2</sup>. The interpretation does not match the data of Lozano *et al*<sup>4</sup>, who report a 10 eV energy deficit from needle emitter spraying EMI-Tf<sub>2</sub>N in pure ion mode. The difference may stem in part from our experimental setup, as we apply the retarding potential to a single grid only and thus cannot guarantee a homogeneous retarding potential across the grid area. Additional details are reported in reference 9.

To confirm pure ion mode operation, time of flight (TOF) mass spectrometry was performed<sup>9</sup> by K. Smith and J. Stark at Queen Mary University of London (QMUL) on the beam emitted from an array of 19 microfabricated capillaries spraying the ionic liquid EMI-BF<sub>4</sub>. Their TOF data in Figure 11 shows two clear steps, corresponding to the atomic mass of the monomer EMI<sup>+</sup> and of the dimer (EMI-BF<sub>4</sub>)EMI<sup>+</sup>. Due to energy losses from the formation of the cusp or jet, the beam potential is not identical to the emitter voltage, especially for the 1300 V curve. This explains why beam current decreases before the corresponding mass is reached. The TOF data shows clearly the absence of droplets, and a beam consisting primarily of ions.

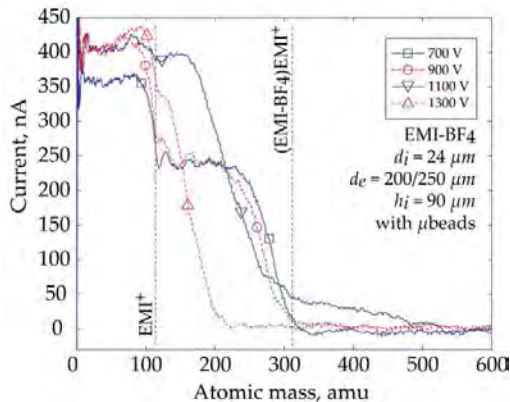


**Figure 11: Time-of-flight traces recorded with a 19-emitter array with capillaries having a 24  $\mu\text{m}$  inner diameter, filled with 5  $\mu\text{m}$  microbeads with an extractor electrode with 200  $\mu\text{m}$  diameter holes spaced at 90  $\mu\text{m}$  from the capillary tip<sup>9</sup>.**

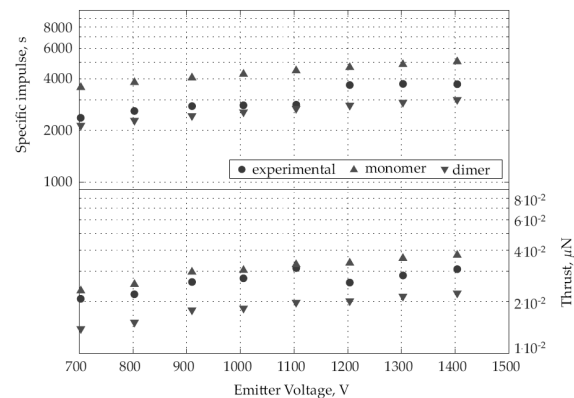


**Figure 12: Plot of the specific impulse and thrust determined from the experimental TOF traces recorded for a 19-emitter array. The experimental data is compared to theoretical values for monomers and dimers of the ionic liquid EMI-BF<sub>4</sub>.**

From the TOF data, the thrust and specific impulse can be computed, as displayed in Figure 12 as a function of extraction voltage. The Isp is 3500 s at 1.2 kV. The computed thrust is 2 pN per emitter, so a total thrust of 300  $\mu$ N could be obtained from a 4" wafer. This thrust represents only a lower limit, as we are not able to collect all the sprayed current in the TOF tests, and are therefore underestimating thrust. We expect also that by further tailoring the flow impedance, we will be able to operate in ionic regime at higher beam currents.

#### IV. Conclusion

We have demonstrated the successful operation of electrospray thrusters consisting of arrays of microfabricated silicon capillaries with integrated extraction electrodes for which we developed a high-yield microfabrication process. To tailor the flow impedance of the capillaries, a post-processing step has been developed in which the capillaries are filled with 5  $\mu$ m diameter microspheres which are fixed inside the capillaries through a silanization process using SiCl<sub>4</sub>.

We have achieved high specific impulse, and shown that the device can work in either pure ion regime or in mixed regime for two ionic liquids depending on flow impedance and applied voltage. The specific impulse has been computed from the TOF traces and is greater than 3500 s for extractor voltages of 1200 V. Stable operation was shown for tens of hours. Such a MEMS thruster is a promising candidate for propulsion systems for formation flying missions as well as for pico- and nano-satellites.

Future work will focus on fabricating larger arrays with thousands of emitters to obtain higher thrust, on lifetime testing, on optimized hydraulic impedance for larger thrust per capillary in ion mode, and on system integration.

#### Acknowledgments

We thank J. Stark and K. Smith of QMUL for very helpful discussions and for the TOF data, and ESA for partial financial support.

#### References

1. Romero-Sanz, R. Bocanegra, J. Fernandez de la Mora, J. "Source of heavy molecular ions based on Taylor cones of ionic liquids operating in the pure ion evaporation regime", *J. Appl. Phys.* 94, 3599-3605, 2003
2. R. Krpoun, "Micromachined Electrospray Thrusters for Spacecraft Propulsion", *PhD thesis*, Ecole Polytechnique Fédérale de Lausanne, No. 4255, 2008.
3. A. Zorzos and P. Lozano, "The Use of Ionic Liquid Ion Sources (ILIS) in FIB Applications" in *Proc. 52nd Int Conf. on Electron, Ion, and Photon Beam Technology and Nanofabrication (Portland)*, 2008
4. P. Lozano, "Energy properties of an EMI-Im ionic liquid ion source", *J. Phys. D: Appl. Phys.* 39, 126-134, 2006
5. R. Krpoun and H. Shea, "Integrated out-of-plane nanoelectrospray thruster arrays for spacecraft propulsion", *Journal of Micromechanics and Microengineering*, 19, p. 045019, 2009
6. P. Griss et al., "Development of micromachined hollow tips for protein analysis based on nanoelectrospray ionization mass spectrometry", *Journal of Micromechanics and Microengineering* 12, pp. 682-687, 2002
7. J. Jhuree, M. S. Alexander, and J. P. W. Stark, Proceedings of the 30<sup>th</sup> International Electric Propulsion Conference, paper #120, Florence, Italy, 2007
8. P. Lozano and M. Martinez-Sanchez, "Electrospray emission from nonwetting flat dielectric surfaces", *J. Colloid Interface Sci.* 280, pp 149-154, 2004
9. R. Krpoun, K. Smith, J. Stark, and H. Shea, "Tailoring the hydraulic impedance of out-of-plane micromachined electrospray sources with integrated electrodes", *Applied Physics Letters*, 94 p163502, 2009
10. M. Gamero-Castaño, *Phys. Fluids* 20, 032103 2008.